Journal of Atmospheric and Solar–Terrestrial Physics 156 (2017) 80–86

Contents lists available at ScienceDirect

Journal of Atmospheric and Solar–Terrestrial Physics

journal homepage: www.elsevier.com/locate/jastp

Some new insights of the characteristics of equatorial plasma bubbles obtained from Indian region

V.L. Narayanan[a,*], S. Gurubaran[b], M.B. Berlin Shiny[c], K. Emperumal[d], P.T. Patil[e]

[a] National Atmospheric Research Laboratory, Gadanki, India
[b] Indian Institute of Geomagnetism, New Panvel, Navi Mumbai, India
[c] 3/78, Periyavilai, Pulippunam, Kanyakumari, India
[d] Equatorial Geophysical Research Laboratory, Indian Institute of Geomagnetism, Tirunelveli, India
[e] MF Radar Facility, Indian Institute of Geomagnetism, Shivaji University Campus, Kolhapur, India

A R T I C L E I N F O

Keywords:
Equatorial plasma bubbles
Airglow imaging
Interdepletion distance
Pre-reversal enhancement

A B S T R A C T

All-sky imaging observations of OI 630.0 nm airglow were carried out in campaign mode from Panhala (16.8°N, 74.1°E geographic; 11.1°N dip latitude), India, during January to March 2008. On 14 of 37 nights, equatorial plasma bubbles were observed. The drift speeds were observed to decrease with time in concurrence with the previous results. The tilts were mostly westward while on rare occasions the plasma bubbles tilted eastwards. The drifts were found to be relatively lesser on disturbed nights while the tilts appear to be marginally larger. The interdepletion distances (or bubble spacings) also showed a decreasing trend with time till midnight indicating that the bubbles approach each other with the passage of time. Such a behavior is not reported earlier and it seems to have important implications for understanding the time evolution of plasma bubbles. On occasions, the bubbles occurred in groups. An ionosonde operating over Indian dip equatorial site Tirunelveli (1.1°N dip latitude) was used to study the variations in the base height of the ionosphere during the plasma bubble observations. The ionosonde measurements indicate lack of significant pre-reversal enhancement (PRE) during geomagnetic quiet days in which the bubbles were observed.

1. Introduction

The formation of ionospheric plasma bubbles over the dip equator after sunset and their extension to the low latitude regions along the geomagnetic field lines constitute an old aeronomical problem to the phenomenon frequently referred to as 'Equatorial spread F' (ESF) (e.g. Makela, 2006; Woodman, 2009 and references therein). The plasma bubbles result from Rayleigh-Taylor instability in the nighttime ionosphere and are associated with electron density irregularities capable of scattering radio waves in a random manner thereby affecting radio communications and navigation systems (Kelley, 2009). The instabilities originate in the bottomside F-region over the dip equator and thereafter grow to higher altitudes as depleted regions of plasma. As an instability feature grows, it spreads to low latitudes away from the dip equator along the geomagnetic field lines. These plasma depleted regions are frequently referred to as equatorial plasma bubbles.

The enhancement in the ionospheric zonal electric field in the evening hours known as pre-reversal enhancement (PRE) and the associated lifting up of bottom side ionosphere known as post sunset rise (PSSR) are believed to be among the most important factors responsible for the onset of ESF (Abdu et al., 1983; Jayachandran et al., 1993; Fejer et al., 1999). However, recent study by Narayanan et al. (2014) indicates that the PRE itself is not significant during the solar minimum period and it does not appear to control the formation of ESF as well.

All-sky imaging of OI 630.0 nm airglow is a powerful technique that is used to study the evolution of plasma bubbles, which manifest themselves as intensity depletions in the airglow images (e.g., Makela, 2006). Parameters like interdepletion distances, drift speeds, tilt with geomagnetic meridian and the width of the bubbles can be determined from all-sky images (E.g. Mendillo and Tyler, 1983; Sinha and Raizada, 2000; Martinis et al., 2003; Pimenta et al., 2003; Makela et al., 2010). In a majority of the past statistical studies, much importance was given to the zonal drift of the bubbles representing the nocturnal ionospheric plasma drift. However, other parameters like interdepletion distances need to be studied in detail as they might give information regarding the nature of the seed perturbations.

In this study, optical observations of equatorial plasma bubbles over the Indian region during January to March 2008 are reported. In addition to discussing the nature of the measured parameters of the

* Correspondence to: National Atmospheric Research Laboratory, Gadanki – 517 112, Andhra Pradesh, India.
E-mail address: narayananvlwins@gmail.com (V.L. Narayanan).

http://dx.doi.org/10.1016/j.jastp.2017.03.006
Received 22 August 2016; Received in revised form 9 March 2017; Accepted 11 March 2017
Available online 12 March 2017
1364-6826/

bubbles (interdepletion distances, drift speeds and tilts), we also point towards the implications of interdepletion distance distribution with time. We discuss about the clustering nature of bubbles. Also the tilts were observed to be larger during geomagnetically disturbed nights compared to that of the quiet nights. Further, we study the variation of ionospheric bottomside heights on the nights of plasma bubble occurrence using an ionosonde situated over Tirunelveli (8.7°N, 77.8°E geographic; 1.1°N dip latitude), a dip equatorial station. The analysis reveals that on these nights PRE was weak or non-existent during geomagnetically quiet periods. In addition to the new insights described herein, first observations of the shrinking of equatorial plasma bubbles (Narayanan et al., 2016a) and direct observations of merging of individual plasma bubbles (Narayanan et al., 2016b) were recently reported based on this campaign data from India.

2. Database

We study the characteristics of plasma bubbles obtained from the OI 630.0 nm imaging observations made at Panhala (16.8°N, 74.1°E geographic; 11.1°N dip latitude) during January to March 2008. The observations were carried out at Panhala in campaign mode by Indian Institute of Geomagnetism. The observations were made with a ~2.4 nm bandwidth interference filter centered at a wavelength of 629.9 nm. A detailed description of the instrument used for the present observations was given by Narayanan et al. (2009). The information regarding the method of data acquisition during the campaign and the details of data analysis was presented in Narayanan et al., (2011, 2013).

Optical observations were made on 37 moonless clear sky nights during the three months mentioned above. On 14 of the 37 nights, intensity depletions extending from the southern horizon to the north of the images were noticed in the OI 630.0 nm images. These features were identified as signatures of plasma bubbles and were considered for further analysis. We use the 3 hourly a_p index to identify geomagnetically quiet and disturbed days. If the maximum value of the 3-hourly a_p index for a day was greater than 12, the day was considered as a disturbed day. Among the 14 nights on which plasma bubbles were observed, seven days were geomagnetically quiet and the remaining seven days were geomagnetically disturbed as given in Table 1.

The images were unwarped and projected in equidistance grids as described in Narayanan et al. (2009). Parameters like drift speed and interdepletion distance were estimated using the cross sections extracted across the bubbles in the east-west direction from the equidistance projection. An example of the raw image, its equidistance projection and the extracted cross-section are shown in Fig. 1. The rectangular area in Fig. 1(b) indicates the region over which all columns of pixel intensities were averaged to obtain the intensity cross-section shown in Fig. 1(c). The distance between adjacent depletions in the cross-sections were measured from several different images containing a bubble pair and averaged to obtain the interdepletion distance or bubble spacing. By obtaining the zonal displacement of a particular intensity depletion in the cross-sections of several different images and from their respective time gaps, the drift speeds were computed. To measure the thickness of the bubbles, only those intensity depletions showing clear wall-like enhancements on both the sides were considered. The westward or eastward tilts were measured only for those bubbles that were extended as a single depleted channel in the images. Bubbles with complex structures like bifurcation features were not considered for tilt measurements. When a line is drawn along the clear portion of a depletion, its tilt from the geomagnetic north would then be equivalent to the vertical tilt of the depletions over the dip equator.

Table 1
Properties of observed plasma bubbles.

Days (Year: 2008)	Max a_p index	Quiet/ Disturbed	Total no. of bubbles	Time of first observation of bubbles (IST)	Groups of bubbles
Jan 1	6	Q	19	20:23	1–19
Jan 4	6	Q	8	20:36	1–2, 3–8
Jan 5	19	D	2	19:59	1–2
Jan 6	22	D	9	20:06	1, 2–9
Jan 11	6	Q	6	22:50	1–5, 6
Jan 12	27	D	4	22:36	1–3
Jan 13	18	D	2	26:02	1–2
Feb 3	22	D	6	20:36	1–6
Feb 4	12	Q	4	20:53	1, 2–4
Feb 5	7	Q	16	21:08	1–16
Feb 6	9	Q	7	21:53	1–7
Feb 10	39	D	3	22:13	1–3
Mar 6	5	Q	5	24:33	1, 2–3, 4,5
Mar 8	27	D	10	20:32	1–10
Total	–	–	101	–	–

Ionosonde measurements from Tirunelveli (8.7°N, 77.8°E geographic; 1.1°N dip latitude) were used to infer the background ionospheric conditions over the dip equator on these nights. The instrument is a Canadian Advanced Digital Ionosonde (CADI) operating in the vertical incidence mode (MacDougall et al., 1993). Further details regarding the system at Tirunelveli are given in Narayanan et al. (2014). Soundings are made once in 15 min during the period considered here. We briefly discuss about the pre-reversal enhancement on the nights of occurrence of plasma bubbles using the F-region base height measurements from ionosonde observations. A schematic map of the airglow observation site depicting the area covered by the imager field of view (FOV) of ~140° at 250 km altitude, the location of the ionosonde and the location of the dip equator is given in Fig. 2.

3. Results and discussion

Being instability features, the plasma bubbles are carried by the background ionospheric plasma whose drift speed is expected to match the thermospheric zonal wind speed when the F-region dynamo is fully operational (Chapagain et al., 2013; Fukushima et al., 2015). Consequently, the tilts of the plasma bubbles are attributed to the altitudinal shears in the plasma drift, probably caused by a combination of meridional shear of the neutral zonal wind and the variations in ionospheric conductivity (Zalesak et al., 1982; Anderson and Mendillo, 1983; Mendillo and Tyler, 1983; Sekar and Kelley, 1998; Makela and Kelley, 2003).

Fig. 3(a) shows the mean drift speeds of the observed plasma bubbles over time (in Indian Standard Time (IST = Universal time +5.5 h)). The vertical bars represent the standard deviations of the estimates made within the corresponding hour. As can be seen, the magnitude of the eastward drifts during quiet periods increases till ~23:30 IST and then decreases as the night progresses. Though there is a delay of about 1 h in the time of maximum eastward drift, the pattern is consistent with observations and model predictions shown in earlier works (Martinis et al., 2003; Arruda et al., 2006; Kishore and Mukherjee, 2007; Chapagain et al., 2012; Taori and Sindhya, 2014). During disturbed nights, it may be noted that the drifts are comparatively lower and are showing only a decreasing trend. The initial increase in eastward drift speeds in pre-midnight hours are not pronounced as during quiet times. Fig. 3(b) shows individual drift speed determinations made every hour. The drifts were mostly eastwards except on one occasion when westward drift motion was observed. Earlier, westward drifts were observed on rare occasions as discussed by Paulino et al. (2010). The observed differences between the drifts obtained during quiet and disturbed periods might be due to the weakening of the F-region dynamo caused by disturbed thermospheric winds.

The observed tilts in the plasma bubbles are shown in Fig. 4. These tilts were calculated with respect to geomagnetic north and hence they

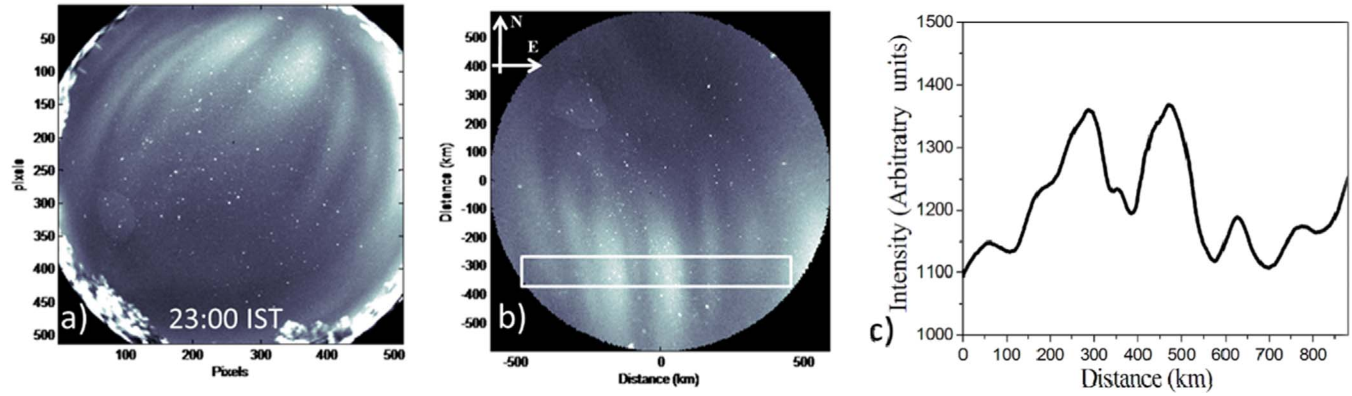

Fig. 1. Examples of a) raw OI 630.0 nm image, b) equidistance projection and c) the extracted cross section corresponding to the rectangle in Fig. 1(b). The image is taken at 23:00 IST on the night of 5 February 2008.

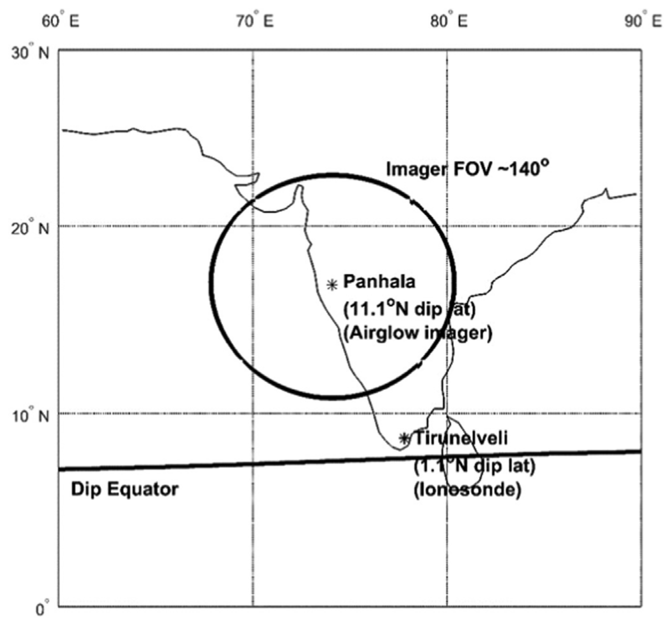

Fig. 2. Schematic showing the sites of airglow imager and ionosonde, approximate area covered in the images for FOV of 140° and the location of dip equator.

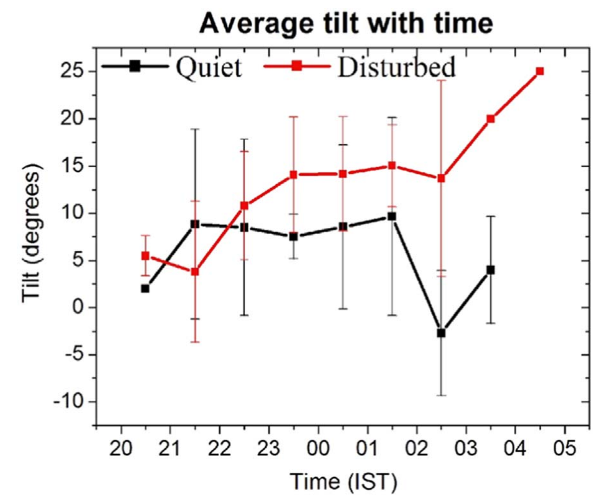

Fig. 4. Observed tilts with time. Positive values correspond to the westward tilts and negative to the eastward tilts (refer to the internet version for colors).

correspond to the tilts of the bubbles from the magnetic meridian at zenith. Earlier studies have revealed an increase in the westward tilt of the plasma bubbles with time (Mendillo and Tyler, 1983; Makela and Kelley, 2003). Since the vertical shears in the zonal drifts are believed to cause the tilts, the longer a bubble spends in the shear, the more is expected to be its tilt. Fig. 4 shows the mean tilt with time. Tilts are found to be relatively larger during geomagnetically disturbed conditions than during quiet conditions. With time, an increase in the magnitude of tilts may be noted from Fig. 4 till 01 IST, particularly during disturbed periods. Since the number of bubbles observed after 01 IST is less during quiet times, the dip in the value of tilts after 01

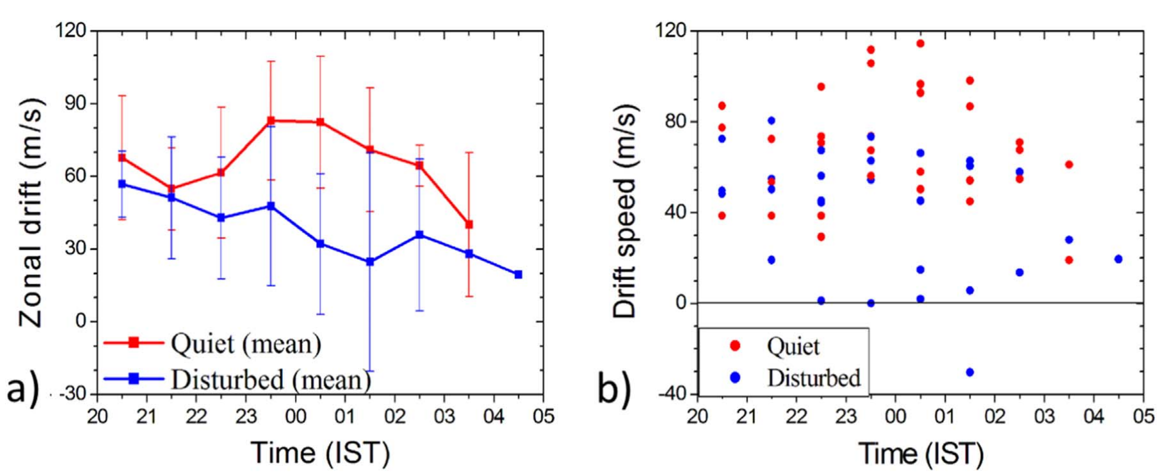

Fig. 3. Observed zonal drift speeds. a) Average values with time. Vertical bars represent standard deviation. b) Individual measurements during quiet and disturbed periods (refer to the internet version of the article for colors).

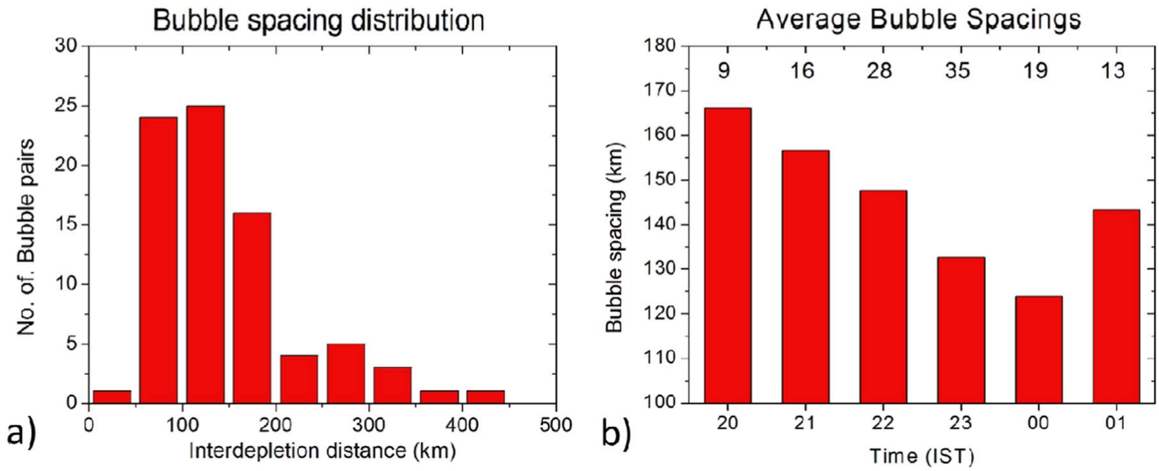

Fig. 5. a) Distribution of bubble spacing, b) Average bubble spacing with time. The numbers on the top indicate number of measurements made during the one hour period.

IST during quiet times might not reflect the true trend. Rather, it could have been due to the constraint posed by the presence of a fewer bubbles then. On the other hand, relatively more number of post-midnight bubbles were observed during disturbed periods. The observation of relatively larger tilts during disturbed conditions indicates that probably altitudinal shears in the plasma drifts are stronger in disturbed periods compared to the quiet periods.

The interdepletion distance or bubble spacing is an important parameter that is believed to reveal information on the scale size of the seed perturbations. Fig. 5(a) shows the distribution of observed spacing between the bubbles. It may be seen that the interdepletion distances were often observed to be within 50–200 km. These values are comparable to the past results (Takahashi et al., 2009; Makela et al., 2010).

From Fig. 5(a) it is clear that most of the bubbles are separated within 200 km distance from the adjacent bubbles. However, on occasions the bubbles are observed to occur in groups wherein a closely spaced set of bubbles is separated with another set or a single bubble with a larger spatial interval. There are also occasions when new bubbles are noticed after the passage of one set of bubbles. Such groupings are listed in the last column of Table 1 by categorizing those bubbles separated by distances greater than about 350 km as different groups. The limit of 350 km is tentatively fixed based on the distribution of the observed bubble spacing during this campaign period as shown in Fig. 5(a), which showed that most of the bubbles were separated within 200 km distance. Therefore, the value may be different for different solar epochs. Such a grouping behavior was already noticed in the case study presented by Narayanan et al. (2012). The interaction of long and short wavelength waves triggering bubbles within the upwelling region of the long wavelength mode might give rise to the clustering nature of the bubbles. The bubble spacing might correspond to the scale size of the shorter scale waves (Sekar et al., 2001). Thus, observation of grouping behavior may support the hypothesis of multiple wave modes giving rise to the formation of plasma bubbles more effectively (Sekar et al., 2001; Narayanan et al., 2012). Such grouping behavior of plasma bubbles has not received enough attention till now. However, they can be useful in understanding the seeding mechanisms in detail.

Fig. 5(b) shows the mean interdepletion distances with time of the night. Note that the measured interdepletion distance for a bubble pair is the average value for the duration of observation of the bubble pair. Therefore, we include the measured value in those hourly bins in which the bubble pair is observed. The number at the top axis in Fig. 5(b) indicates the number of bubble pairs observed within the 1 h bin. The plot reveals a general trend of about 10 km decrease in the average value of bubble spacing between successive hours till midnight. This might be due to the decreasing ionospheric plasma drift speeds with time. Since the eastward drift speeds of the bubbles generated earlier may decrease as they move to later local time zones (i.e. farther eastern longitudes), the trailing bubbles may approach the leading ones with relatively larger drift speeds. While observing from a fixed location, this might be seen as a reduction in the interdepletion distances as shown in Fig. 5(b). This may sometimes lead to the merging of the individual bubbles at late night hours as shown in Narayanan et al. (2016b). Indeed, merging of individual plasma bubbles is gaining attention in recent years (Huang et al., 2011; Huba et al., 2015; Narayanan et al., 2016b).

At the same time, it might be noticed that there is a relative enhancement in the average interdepletion distance value at 01:00 UT in Fig. 5(b). Though the exact cause of the increase is not known, there may be some reasons as described below. In a recent study, some of the plasma bubbles were observed to shrink and disappear during the course of the night (Narayanan et al., 2016a). It was also noticed in Narayanan et al. (2016a) that one bubble may shrink while the adjacent one does not. Such shrinking of some of the bubbles would have resulted in their disappearance producing a larger distance between adjacent bubbles in the later hours. On the other hand, the increase might be due to generation of fresh bubbles in the post-midnight hours (Patra et al., 2009). To our knowledge, such an analysis of time variation in bubble spacing has not been carried out earlier and it needs to be carried out with a larger dataset to reconfirm the findings presented herein.

Fig. 6 shows the distribution of width or thickness of the bubbles observed. As already mentioned, only those bubbles whose eastern and western walls were clearly seen in the extracted cross-sections were used to measure the thickness. While the bubble spacing renders insight on the nature of seed perturbation, the width is the true zonal extent of the plasma bubble. It may be seen in Fig. 6 that most of the bubbles have had thicknesses ranging between 20 and 80 km. On the average, the bubbles had a width of ~60 km. This value is in agreement with the simulation studies of Huba et al. (2009) and earlier radar observations of Tsunoda et al. (1982).

Many of the earlier studies on initiation of the ESF have shown that PRE plays a determining role in the formation of instabilities (Abdu et al., 1983; Fejer et al., 1999). The PRE is known to be stronger during high solar activity periods (Oyekola and Oluwafemi, 2008) than during low solar activity periods. However, the studies during the solar minimum period often indicate that plasma bubbles (or ESF) are generated during post-midnight hours (Patra et al., 2009) or on the nights without significant PRE (Narayanan et al., 2014). Therefore, identifying the extent of the control by the PRE in initiating ESF during different solar activity conditions is important.

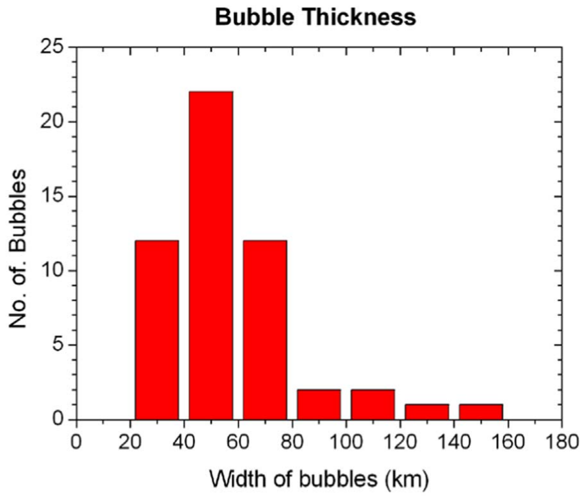

Fig. 6. Observed mean width of the depletions.

Data from coincident ionosonde measurements made from Tirunelveli in the Indian sector are used to understand the background conditions responsible for the initiation of plasma bubbles during the days of optical observations discussed herein. Fig. 7(a) shows the F-layer base height variations during geomagnetically quiet days. The dotted line shows the sunset time in the corresponding F-region altitudes and the arrow indicates the time of first observation of a plasma bubble in a night. From Fig. 7(a), it may be inferred that except 1 January 2008, no other quiet days possessed significant height rise above about 300 km associated with the PRE. Especially the two days 4 January and 4 February 2008 did not show any signature of PRE, but still bubbles were observed on both days before 21:00 IST itself (see Table 1 and arrows in Fig. 7(a)). This observation indicates that plasma bubbles could form without strong PRE during low solar activity conditions.

Fig. 7(b) shows the base height measurements during magnetically disturbed days. A comparison of Fig. 7(b) and Table 1 indicates that during magnetically disturbed times, the plasma bubbles were observed shortly after the base height rose above 280 km. The only exception to this feature in the current dataset was noticed on 10 February 2008. This is in contrast to the quiet period observations shown in Fig. 7(a), wherein the maximum heights attained were confined below 280 km in most of the cases. We caution here that we do not emphasize anything particular about 280 km level, but refer to it in order to point out the differences in the extent of lifting up of the ionosphere during quiet and disturbed periods. The observations suggest that during magnetically quiet periods the upliftment associated with the PRE does not seem to play any determining role in the formation of plasma bubbles during low solar activity periods. However, during disturbed conditions of the low solar activity periods, the ionosphere might experience larger upliftments than the quiet periods, which could have facilitated the formation of plasma bubbles.

The growth rate of the Rayleigh-Taylor instability that produces plasma bubbles is inversely proportional to the ion-neutral collision frequency (e.g. Kelley, 2009). The ion-neutral collision frequency is dependent of the neutral densities and hence it decreases exponentially with altitude (e.g. Rishbet and Garriott, 1969). When the bottomside ionosphere is lifted to the higher altitudes due to the PRE, the neutral

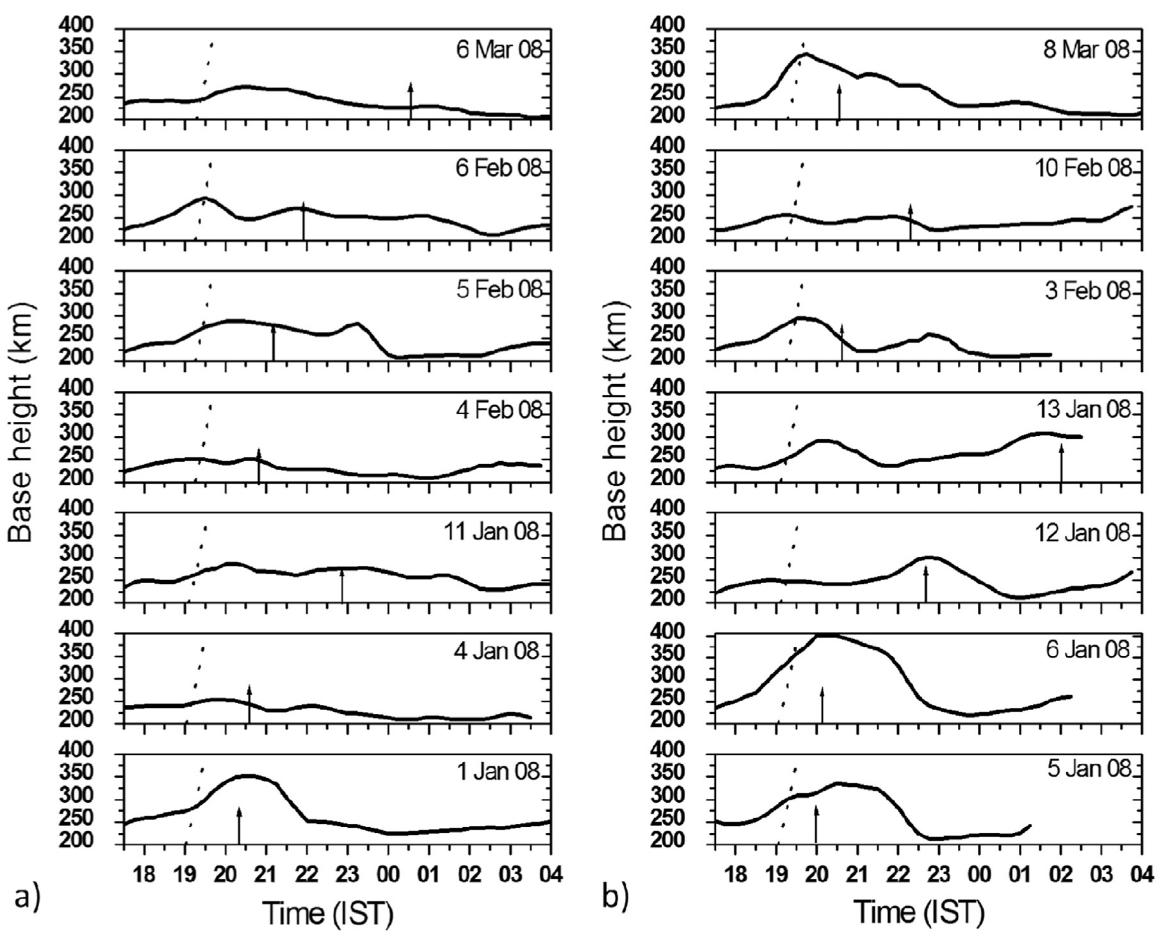

Fig. 7. The ionospheric base height measurements from Tirunelveli during a) quiet days, b) magnetically disturbed days. The arrows indicate the first observation of a plasma bubble in the imager. The dotted lines indicate F-region sunset.

density is relatively lesser resulting in smaller ion-neutral collision frequency and larger probability of plasma bubble growth. During high and medium solar activity periods, the thermospheric neutral density is higher compared to that of the low solar activity periods (Emmert and Picone, 2010). Therefore, during solar minimum periods the ion-neutral collision frequency decreases to a good extent in the lower F-region ionosphere itself. We emphasize here that the observations discussed in this work are taken during 2008, a year of unusual low solar activity resulting in reduced thermospheric mass densities (Emmert et al., 2010). Therefore during the period of observations, in spite of lack of the PRE, the background ionosphere would have been supportive for the formation of plasma bubbles due to low ion-neutral collision frequencies. In addition, other factors like stronger seeding and vertical winds would have played a role in the generation of plasma bubbles without PRE of reasonable magnitudes.

4. Summary and conclusions

In this work we have presented results from observations carried out during a three-month campaign between January and March 2008. The observations were made over the low latitude Indian site, Panhala, with an all-sky airglow imager monitoring OI 630.0 nm emission. Observations on 14 out of 37 clear sky nights revealed the presence of plasma bubbles seen as airglow depletions. We had separated those nights into geomagnetically quiet and disturbed based on a_p indices as described in Section 2 and the characteristics of plasma bubbles were studied. Supporting ionosonde data were available from the dip equatorial site, Tirunelveli, to study the ambient bottomside ionospheric conditions. We summarize our findings below.

1. The zonal drift of the plasma bubbles was eastward and its magnitude decreases with time during the course of the night. The magnitude of the drifts was relatively smaller during disturbed periods.
2. The observed tilts during disturbed conditions were generally higher than those during quiet periods suggesting stronger vertical shears in the zonal plasma flow during disturbed conditions.
3. The interdepletion distances or the bubble spacings are typically between 50 and 200 km, though there was a decreasing trend noticed during the course of the night. The latter feature indicates that the bubbles rather approach each other with time, which may lead to an eventual merging in some cases.
4. The average width of the bubbles was ~60 km.
5. The uplifting of the bottomside ionosphere due to PRE was not significant during quiet periods, though the plasma bubbles were still observed on several nights. Here, it may be noted that the observations are made during unusually low solar activity conditions of 2008. It is possible that the ion-neutral collision frequencies would have dropped significantly so that the plasma bubbles were generated without strong PRE.

Many aspects of this study are new and call for further detailed investigation. Especially, the observations of the decreasing trend of bubble spacing during the course of a night, the difference in tilts between quiet and disturbed nights and the absence of PRE during the periods when the bubbles are generated need greater attention.

Acknowledgements

The lead author V.L.N. acknowledges support from the INSPIRE Faculty Award from Department of Science and Technology, Government of India. The data used in this work were acquired by Indian Institute of Geomagnetism with the support of Department of Science and Technology, Government of India. Though data cannot be publicly shared, data requests can be made and access to data will be provided according to the Institute's data sharing policy in place. Person to contact for imaging and ionosonde data is S.G.

References

Abdu, M.A., de Medeiros, R.T., Bittencourt, J.A., Batista, I.S., 1983. Vertical ionization drift velocities and range type spread F in the evening equatorial ionosphere. J. Geophys. Res. 88, 399–402.
Anderson, D.N., Mendillo, M., 1983. Ionospheric conditions affecting the evolution of equatorial plasma depletions. Geophys. Res. Lett. 10, 541–544.
Arruda, D.C.S., Sobral, J.H.A., Abdu, M.A., Castilho, V.M., Takahashi, H., Medeiros, A.F., Buriti, R.A., 2006. Theoretical and experimental zonal drift velocities of the ionospheric plasma bubbles over the Brazilian region. Adv. Space Res. 38, 2610–2614.
Chapagain, N.P., Fisher, D.J., Meriwether, J.W., Chau, J.L., Makela, J.J., 2013. Comparison of zonal neutral winds with equatorial plasma bubble and plasma drift velocities. J. Geophys. Res. Space Phys. 118, 1802–1812. http://dx.doi.org/10.1002/jgra.50238.
Chapagain, N.P., Taylor, M.J., Makela, J.J., Duly, T.M., 2012. Equatorial plasma bubble zonal velocity using 630.0 nm airglow observations and plasma drift modeling over Ascension Island. J. Geophys. Res. 117, A06316. http://dx.doi.org/10.1029/2012JA017750.
Emmert, J.T., Lean, J.L., Picone, J.M., 2010. Record-low thermospheric mass density during the 2008 solar minimum. Geophys. Res. Lett. 37, L12102. http://dx.doi.org/10.1029/2010GL043671.
Emmert, J.T., Picone, J.M., 2010. Climatology of globally averaged thermospheric mass density. J. Geophys. Res. 115, A09326. http://dx.doi.org/10.1029/2010JA015298.
Fejer, B.G., Scherliess, L., de Paula, E.R., 1999. Effects of the vertical plasma drift velocity on the generation and evolution of equatorial spread F. J. Geophys. Res. 104, 19859–19869.
Fukushima, D., Shiokawa, K., Otsuka, Y., Nishioka, M., Kubota, M., Tsugawa, T., Nagatsuma, T., Komonjinda, S., Yatini, C.Y., 2015. Geomagnetically conjugate observation of plasma bubbles and thermospheric neutral winds at low latitudes. J. Geophys. Res. Space Phys. 120, 2222–2231. http://dx.doi.org/10.1002/2014JA020398.
Huang, C.-S., de La Beaujardiere, O., Roddy, P.A., Hunton, D.E., Pfaff, R.F., Valladares, C.E., Ballenthin, J.O., 2011. Evolution of equatorial ionospheric plasma bubbles and formation of broad plasma depletions measured by the C/NOFS satellite during deep solar minimum. J. Geophys. Res. 116, A03309. http://dx.doi.org/10.1029/2010JA015982.
Huba, J.D., Krall, J., Joyce, G., 2009. Atomic and molecular ion dynamics during equatorial spread F. Geophys. Res. Lett. 36, L10106. http://dx.doi.org/10.1029/2009GL037675.
Huba, J.D., Wu, T.W., Makela, J.J., 2015. Electrostatic reconnection in the ionosphere. Geophys. Res. Lett. 42, 1626–1631. http://dx.doi.org/10.1002/2015GL063187.
Jayachandran, B., Balan, N., Rao, P.B., Sastri, J.H., Bailey, G.J., 1993. HF Doppler and ionosonde observations on the onset conditions of equatorial spread F. J. Geophys. Res. 98, 13741–13750.
Kelley, M.C., 2009. The Earth's Ionosphere: plasma Physics and Electrodynamics. Academic Press, Singapore.
Kishore, H.M., Mukherjee, G.K., 2007. Equatorial F-region plasma drifts: a study using OI 630 nm emission all-sky images. Curr. Sci. 93, 488–497.
MacDougall, J. W., Grant, I. F., Shen, X, 1993. The Canadian advanced digital ionosonde: design and results. Proceedingns of Session G6, 24th General Assembly of the International Union of Radio Science (URSI), Kyoto, Japan. http://www.sws.bom.gov.au/IPSHosted/INAG/uag-104/text/macdoug.html.
Makela, J.J., 2006. A review of imaging low-latitude ionospheric irregularity processes. J. Atmos. Sol.-Terr. Phys. 68, 1441–1458.
Makela, J.J., Kelley, M.C., 2003. Field-aligned 777.4-nm composite airglow images of equatorial plasma depletions. Geophys. Res. Lett. 30, 1442. http://dx.doi.org/10.1029/2003GL017106.
Makela, J.J., Vadas, S.L., Muryanto, R., Duly, T., Crowley, G., 2010. Periodic spacing between consecutive equatorial plasma bubbles. Geophys. Res. Lett. 37, L14103. http://dx.doi.org/10.1029/2010GL043968.
Martinis, C., Eccles, J.V., Baumgardner, J., Manzano, J., Mendillo, M., 2003. Latitude dependence of zonal plasma drifts obtained from dual-site airglow observations. J. Geophys. Res. 108, 1129. http://dx.doi.org/10.1029/2002JA009462.
Mendillo, M., Tyler, A., 1983. Geometry of depleted plasma regions in the equatorial ionosphere. J. Geophys. Res. 88, 5778–5782.
Narayanan, V.L., Gurubaran, S., Emperumal, K., 2009. Imaging observations of upper mesospheric nightglow emissions from Tirunelveli (8.7°N). Indian J. Radio Space Phys. 38, 150–158.
Narayanan, V.L., Gurubaran, S., Emperumal, K., Patil, P.T., 2011. Unusual optical observations of OI greenline during a geospace event on 1 February 2008. J. Geophys. Res. 116, A09315. http://dx.doi.org/10.1029/2010JA016339.
Narayanan, V.L., Taori, A., Patra, A.K., Emperumal, K., Gurubaran, S., 2012. On the importance of wave-like structures in the occurrence of equatorial plasma bubbles: a case study. J. Geophys. Res. 117, A01306. http://dx.doi.org/10.1029/2011JA017054.
Narayanan, V.L., Gurubaran, S., Emperumal, K., Patil, P.T., 2013. A study on the night time equatorward movement of ionization anomaly using thermospheric airglow imaging technique. J. Atmos. Sol.-Terr. Phys. 103, 113–120. http://dx.doi.org/10.1016/j.jastp.2013.03.028.
Narayanan, V.L., Sau, S., Gurubaran, S., Shiokawa, K., Balan, N., Emperumal, K., Sripathi, S., 2014. A statistical study of satellite traces and evolution of equatorial spread F. Earth Planets Space 66, 160. http://dx.doi.org/10.1186/s40623-014-

0160-4.
Narayanan, V.L., Gurubaran, S., Shiokawa, K., Emperumal, K., 2016a. Shrinking equatorial plasma bubbles. J. Geophys. Res. – Space Phys. 121. http://dx.doi.org/10.1002/2016JA022633.
Narayanan, V.L., Gurubaran, S., Shiokawa, K., 2016b. Direct observational evidence for the merging of equatorial plasma bubbles. J. Geophys. Res. – Space Phys. 121. http://dx.doi.org/10.1002/2016JA022861.
Oyekola, O.S., Oluwafemi, C.O., 2008. Solar and geomagnetic trends of equatorial evening and nighttime F region vertical ion drifts. J. Geophys. Res. 113, A12318. http://dx.doi.org/10.1029/2008JA013315.
Patra, A.K., Phanikumar, D.V., Pant, T.V., 2009. Gadanki radar observations of F region field-aligned irregularities during June solstice of solar minimum: first results and preliminary analysis. J. Geophys. Res. 114, A12305. http://dx.doi.org/10.1029/2009JA014437.
Paulino, I., Medeiros, A.F., Buriti, R.A., Sobral, J.H.A., Takahashi, H., Gobbi, D., 2010. Optical observations of plasma bubble westward drifts over Brazilian tropical region. J. Atmos. Sol.-Terr. Phys. 72, 521–527. http://dx.doi.org/10.1016/j.jastp.2010.01.015.
Pimenta, A.A., Bittencourt, J.A., Fagundes, P.R., Sahai, Y., Buriti, R.A., Takahashi, H., Taylor, M.J., 2003. Ionospheric plasma bubble zonal drifts over the tropical region: a study using OI 630 nm emission all-sky images. J. Atmos. Sol.-Terr. Phys. 65, 1117–1126.
Rishbet, H., Garriott, O.K., 1969. Introduction to Ionospheric Physics. Academic Press, Amsterdam.
Sekar, R., Kelley, M.C., 1998. On the combined effects of vertical shear and zonal electric field patterns on nonlinear equatorial spread F evolution. J. Geophys. Res. 103, 20735–20747.
Sekar, R., Kherani, E.A., Rao, P.B., Patra, A.K., 2001. Interaction of two long-wavelength modes in the nonlinear numerical simulation model of equatorial spread F. J. Geophys. Res. 106, 24765–24775.
Sinha, H.S.S., Raizada, S., 2000. Some new features of ionospheric plasma depletions over the Indian zone using all sky optical imaging. Earth Planets Space 52, 549–559.
Takahashi, H., Taylor, M.J., Pautet, P.-D., Medeiros, A.F., Gobbi, D., Wrasse, C.M., Fechine, J., Abdu, M.A., Batista, I.S., Paula, E., Sobral, J.H.A., Arruda, D., Vadas, S.L., Sabbas, F.S., Fritts, D.C., 2009. Simultaneous observation of ionospheric plasma bubbles and mesospheric gravity waves during the SpreadFEx Campaign. Ann. Geophys. 27, 1477–1487.
Taori, A., Sindhya, A., 2014. Measurements of equatorial plasma depletion velocity using 630 nm airglow imaging over a low-latitude Indian station. J. Geophys. Res. – Space Phys. 119, 396–401. http://dx.doi.org/10.1002/2013JA019465.
Tsunoda, R.T., Livingston, R.C., McClure, J.P., Hanson, W.B., 1982. Equatorial plasma bubbles: Vertically elongated wedges from the bottomside F layer. J. Geophys. Res. 87, 9171–9180.
Woodman, R.F., 2009. Spread F – an old equatorial aeronomy problem finally resolved? Ann. Geophys. 27, 1915–1934.
Zalesak, S.T., Ossakow, S.L., Chaturvedi, P.K., 1982. Nonlinear equatorial spread F: the effect of neutral winds and background Pedersen conductivity. J. Geophys. Res. 87, 151–166.